1-1-2015

Uncertainty management in multiobjective hydro-thermal self-scheduling under emission considerations

Jamshid Aghaei
Shiraz University of Technology, jamshid@uow.edu.au

Abdollah Ahmadi
University of New South Wales

Abdorreza Rabiee
Shahrekord University, rabiee@iust.ac.ir

Vassilios G. Agelidis
University of New South Wales

Kashem M. Muttaqi
University of Wollongong, kashem@uow.edu.au

See next page for additional authors

Uncertainty management in multiobjective hydro-thermal self-scheduling under emission considerations

Abstract

In this paper, a stochastic multiobjective framework is proposed for a day-ahead short-term Hydro Thermal Self-Scheduling (HTSS) problem for joint energy and reserve markets. An efficient linear formulations are introduced in this paper to deal with the nonlinearity of original problem due to the dynamic ramp rate limits, prohibited operating zones, operating services of thermal plants, multi-head power discharge characteristics of hydro generating units and spillage of reservoirs. Besides, system uncertainties including the generating units' contingencies and price uncertainty are explicitly considered in the stochastic market clearing scheme. For the stochastic modeling of probable multiobjective optimization scenarios, a lattice Monte Carlo simulation has been adopted to have a better coverage of the system uncertainty spectrum. Consequently, the resulting multiobjective optimization scenarios should concurrently optimize competing objective functions including GENeration COmpany's (GENCO's) profit maximization and thermal units' emission minimization. Accordingly, the ε-constraint method is used to solve the multiobjective optimization problem and generate the Pareto set. Then, a fuzzy satisfying method is employed to choose the most preferred solution among all Pareto optimal solutions. The performance of the presented method is verified in different case studies. The results obtained from ε-constraint method is compared with those reported by weighted sum method, evolutionary programming-based interactive Fuzzy satisfying method, differential evolution, quantum-behaved particle swarm optimization and hybrid multi-objective cultural algorithm, verifying the superiority of the proposed approach.

Keywords

management, multiobjective, hydro, uncertainty, thermal, considerations, self, scheduling, under, emission

Disciplines

Engineering | Science and Technology Studies

Publication Details

J. Aghaei, A. Ahmadi, A. Rabiee, V. G. Agelidis, K. M. Muttaqi & H. A. Shayanfar, "Uncertainty management in multiobjective hydro-thermal self-scheduling under emission considerations," Applied Soft Computing Journal, vol. 37, pp. 737-750, 2015.

Authors

Jamshid Aghaei, Abdollah Ahmadi, Abdorreza Rabiee, Vassilios G. Agelidis, Kashem M. Muttaqi, and H A. Shayanfar

Uncertainty Management in Multiobjective Hydro-Thermal Self-scheduling under Emission Considerations

Jamshid Aghaei[1], Abdollah Ahmadi[2], Abdorreza Rabiee[3], Vassilios G. Agelidis[2], Kashem M. Muttaqi[4], and H. A. Shayanfar[5]

[1]Department of Electrical and Electronics Engineering, Shiraz University of Technology

[2]The Australian Energy Research Institute and the School of Electrical Engineering and Telecommunications, the University of New South Wales, Sydney, 2052, NSW, Australia

[3]Department of Electrical Engineering, Faculty of Technology and Engineering, Shahrekord University

[4]Integral Energy Power Quality and Reliability Centre, School of Electrical, Computer and Telecommunications Engineering, University of Wollongong

[5]Center of Excellence for Power System Automation and Operation, Department of Electrical Engineering, Iran University of Science and Technology, Tehran, Iran

Corresponding Author:J. Aghaei, Department of Electrical and Electronic Engineering, Shiraz University of Technology, Modars Blvd. Shiraz, Iran. P.O. 71555-313, Tel.: (+98)-(912)-(586 5573); Fax: (+98)-(0711)-(7353502); E-mail address: aghaei@sutech.ac.ir.

Abstract- In this paper, a stochastic multiobjective framework is proposed for a day-ahead short-term Hydro Thermal Self-Scheduling (HTSS) problem for joint energy and reserve markets. An efficient linear formulations are introduced in this paper to deal with the nonlinearity of original problem due to the dynamic ramp rate limits, prohibited operating zones, operating services of thermal plants, multi-head power discharge characteristics of hydro generating units and spillage of reservoirs. Besides, system uncertainties including the generating units' contingencies and price uncertainty are explicitly considered in the stochastic market clearing scheme. For the stochastic modeling of probable multiobjective optimization scenarios, a lattice Monte Carlo simulation has been

adopted to have a better coverage of the system uncertainty spectrum. Consequently, the resulting multiobjective optimization scenarios should concurrently optimize competing objective functions including GENeration COmpany's (GENCO's) profit maximization and thermal units' emission minimization. Accordingly, the ε-constraint method is used to solve the multiobjective optimization problem and generate the Pareto set. Then, a fuzzy satisfying method is employed to choose the most preferred solution among all Pareto optimal solutions. The performance of the presented method is verified in different case studies. The results obtained from ε-constraint method is compared with those reported by weighted sum method, evolutionary programming-based interactive Fuzzy satisfying method, differential evolution, quantum-behaved particle swarm optimization and hybrid multi-objective cultural algorithm, verifying the superiority of the proposed approach.

Index Terms— Stochastic Programming, Hydro-Thermal Self Scheduling, Price Uncertainty, Generating Unit Contingency, Multiobjective Mathematical Programming

Nomenclature

Indices

i: Thermal unit index

j: Hydro unit index

t: Time interval (hour) index. For instance, $p(j,t,s)$ is the power output of hydro unit j at hour t in the s^{th} scenario (MW)

s: Scenario index

q: Network area index

Constants

α_k : Probability of k^{th} price level

$\pi^b(t)$: Bilateral contract price ($/MWh)

π^E: Emission Price($/lbs)

Θ : Number of periods in the planning horizon

A_i: Shut-down cost of unit i ($)

A_j: Start-up cost of unit j ($)

$b_n(i)$: Slope of block n of fuel cost curve of unit i ($/MWh)

$b_n(j)$: Slope of the volume block n of the reservoir associated to unit j ($m^3/s/Hm^3$)

$b_n^k(j)$: Slope of the block n of the performance curve k of unit j ($MW/m^3/s$)

$be_n(i)$: Slope of segment n in emission curve of unit i (lbs/MWh)

e_i, f_i : Coefficients of valve loading cost function

$E_{\min}(i)$: Generated emission by off-unit while providing non-spinning reserve (lbs)

$E(p_{n-1}^u(i))$: Generated emission of n-1^{th} upper limit in the emission curve of unit i (lbs)

EGR: Emission group (SO_2 or NO_x)

E^{QUOTA}: Emission quota (lbs)

$F(p_{n-1}^u(i))$: Generation cost of n-1^{th} upper limit in the fuel cost curve of unit i ($/h)

$F(j,t,s)$: Forecasted natural water inflow of the reservoir associated to unit j (Hm^3/h)

L: Number of performance curves

M: Number of prohibited operating zones

NL: Number of blocks of the piecewise linearized start-up fuel function

NP: Number of price levels

NS: Number of scenario after scenario reduction

NA: Number of areas in the network

$p^b(t)$: Power capacity of bilateral contract (MW)

P(s): Probability of scenario s

Pr(s): Normalized probability of scenario s

$p_{min}(i)$, $p_{max}(i)$: Minimum and Maximum power output of unit i (MW)

$\underline{p}_n(j)$: Minimum power output of unit j for performance curve n (MW)

$\bar{p}(j)$: Capacity of unit j (MW)

$p_n^d(i)$: Lower limit of n^{th} prohibited operating zone of unit i (MW)

$p_{n-1}^u(i)$: Upper limit of n-1^{th} prohibited operating zone of unit i (MW)

$\underline{Q}(j), \bar{Q}(j)$:Minimum and Maximum water discharge of unit j (m^3/s)

$RDL_n(i)$, $RUL_n(i)$:Ramp down and Ramp up limit for block n (MW)

$SUE(i)$,$SDE(i)$: Start-up and shut-down emission generated by unit i (lbs)

$SU(i)$,$SD(i)$: Start-up and shut-down ramp rate limit of unit i (MW/h)

$RDL(p(i,t,s))$, $RUL(p(i,t,s))$: Ramping down and ramping up limit of unit i (MW)

$v_0(j)$: Minimum content of the reservoir associated to unit j (Hm^3)

$v_n(j)$: Maximum content of the reservoir j associated to n^{th} performance curve (Hm^3)

Variables

$\delta_n(i,t,s)$: Generation of block n of fuel cost curve for unit i (MW)

$\psi_n(i,t,s)$: Generation of block n of unit i for valve loading effect curve (MW)

$\pi^{sp}(t,s)$, $\pi^{sr}(t,s)$, and $\pi^{ns}(t,s)$: Market price for energy, spinning and non-spinning reserve ($/MWh), respectively

μ_n^r : Individual membership function (the degree of optimality) for the n^{th} objective function in the r^{th} Pareto optimal solution

w_n: The weight factor of the n^{th} objective function in the MMP problem

μ^r : Total membership function of the r^{th} Pareto optimal solution

$B(i,t,s)$: Start-up cost of unit i ($)

$C(i,t,s)$: Valve loading effect cost of unit i ($)

$F(i,t,s)$: Fuel cost of unit i ($)

EP: Main objective function (expected profit of GENCO)

EA: GENCO's total expected profit in dollars after arbitrage

EE: Expected generated emission for each Pareto optimal solution (lbs)

$N_d(i,t,s)$,$N_u(i,t,s)$: Non-spinning reserve of thermal unit i in the spot market when unit is off and on, respectively (MW)

$N_d(j,t,s)$, $N_u(j,t,s)$: Non-spinning reserve of a hydro unit j in the spot market when unit is off and on, respectively (MW)

$p(i,t,s)$: Power output of thermal unit i (MW)

$\bar{p}(i,t,s)$: Maximum power output of unit i (MW)

$p(j,t,s)$: Power output of hydro unit j (MW)

$p^{sp}(t,s)$: Power for bid on the spot market (MW)

$PROFIT(s)$: Profit of scenario s

$q_n(j,t,s)$: Water discharge of hydro unit j and block n (m^3/s)

$R(i,t,s)$, $R(j,t,s)$:Spinning reserve of a thermal unit i and hydro unit j in the spot market (MW), respectively

$v(j,t,s)$: Water content of the reservoir associated with unit j (Hm^3)

Binary variables

$I(i,t,s)$=1 if thermal unit i is on

$I(j,t,s)$ =1 if hydro unit j is on

$I_d(i,t,s)$ =1 if unit i provide non-spinning reserve when unit is off.

$\beta_n(i,t,s)$ =1 if block n of fuel cost curve of unit i is selected

$\beta_n(j,t,s)$ =1 if volume of reservoir water is greater than $v_n(j)$

$\chi_n(i,t,s)$ =1 if power output of unit i has exceeded block n of valve loading effect curve

$W^P_{k,t,s}$: Obtained from the roulette wheel mechanism in the scenario generation stage indicating whether k^{th} price level in the s^{th} scenario occurred ($w^P_{k,t,s}$ =1) or not ($w^P_{k,t,s}$ =0)

$W_{i,t,s}$, $W_{j,t,s}$: Status of the i^{th} thermal and j^{th} hydro unit obtained from LMCS in the scenario generation stage (forced outage state, i.e. W=0 or available, i.e. W=1).

$y(i,t,s)$ =1 if thermal unit i is started-up

$y(j,t,s)$ =1 if hydro unit j is started-up

$z(i,t,s)$ =1 if unit i is shut-down

Sets

I: Thermal units

J: Hydro units

N: Set of indices of blocks of piecewise linearized hydro unit performance curve

NE: The blocks of piecewise linearized thermal unit emission curve

T: The periods of market time horizon T ={1, 2, …, NT}

S: Scenario

I. Introduction

For several years Unit Commitment (UC) has been used to determine the optimal scheduling of power producers for different horizons (daily, weekly and etc.). The Independent System Operator (ISO) implements Security-Constrained Unit Commitment (SCUC) problem that its objective function is minimization of cost while considering system security and meeting system load. GENeration COmpanies (GENCOs) uses Price-Based Unit Commitment (PBUC) to maximize their profit but they are not concerning about providing the system load [1]. The UC and PBUC are respectively termed as the Hydro-Thermal Scheduling (HTS) and Hydro-Thermal Self Scheduling (HTSS) [2] for the system with the hydro and thermal units. Different solution methods of the HTSS problem are comprehensively classified into heuristic and analytical methods in [3]. In [4], a novel mixed-integer nonlinear approach is proposed to solve the short-term hydro scheduling problem in the day-ahead electricity market, considering not only head-dependency, but also start/stop of units, discontinuous operating regions and discharge ramping constraints.

In [5], a stochastic programming formulation is proposed for trading wind energy in a market environment under uncertainty of energy market prices as well as the volatile and intermittent nature of wind energy. Optimal hydro scheduling for the short-term time horizon is proposed in [6] wherein a mixed-integer nonlinear programming framework including the head effect on power production, start-up costs of units, multiple operating regions, and discharge variation constraints is considered. Also in [6], as new contributions to the field, the market price uncertainty is introduced in the model via price scenarios. Also, the risk management is included in [6] using Conditional Value-at-Risk (CVR) to limit profit volatility. In [7], Monte Carlo Simulation (MCS) method is implemented to generate random hourly prices for energy, ancillary services, and fuel in the stochastic PBUC framework. A stochastic midterm risk-constrained hydrothermal scheduling algorithm is proposed for profit maximization of GENCOs in [8]. In [9-10], the stochastic SCUC is implemented for the electricity market clearing problem while reserve services are determined based on the expected-load-not-served. Two methodologies are suggested to reduce computational burden of the stochastic UC in [11]. The stochastic nature of the electricity price is modeled in a multi-stage stochastic framework for thermal units' self-scheduling in [12]. Ref [13] used a deterministic MIP approach for solving the HTSS problem of generating units. Also, [14] presents a mixed-integer stochastic framework for a hydro-wind power system scheduling. Ref. [15] presents the techno-economic factor for distributed generation units based on the effect of their generation on the network

losses. The MCS method is used for the outages of generating units and transmission lines together with the load forecasting inaccuracies in the SCUC problem in [16]. A stochastic self-scheduling for thermal units based on the ARIMA model is utilized in [17]. In [18], an interval-fuzzy two-stage stochastic programming method is developed for the carbon dioxide (CO2) emission trading under uncertainty. It is worth to mention that, in the above-mentioned papers, the valve loading effect and dynamic ramp rate are not taken into account. On the other hand, to the best of our knowledge, no research work in the area considers a stochastic multiobjective multiperiod framework for the HTSS problem. In other words, the uncertainty sources (generating unit contingencies and price forecast uncertainty) have been taken into account in this work. Accordingly, the main contribution of this paper is to present a multiperiod stochastic multiobjective framework for the short term HTSS. In the proposed model, the expected profit is maximized based on the MIP optimization formulation while at the same time the expected emission is minimized in the form of multiobjective stochastic problem. Furthermore, the price uncertainty is considered using the Probability Distribution Function (PDF) of price forecast error. Concurrently, the roulette wheel mechanism is implemented to generate the price of energy and spinning/non-spinning reserve for each hour and Lattice Monte Carlo simulation (LMCS) method is applied to consider Forced Outage Rate (FOR) of units. For the sake of accuracy, more practical constraints of thermal and hydro units are taken into account. In [19-21], the valve loading effect cost is modeled in the form of a nonlinear sinusoidal function which is linearized in our framework. Based on the work [22], different dynamic ramp rate is also proposed in the HTSS framework. Finally, a general formulation is recommended for the multi-performance curve of hydro units based on [23]. Different solution methods for the optimization problem can be found in [24-27]. Accordingly, the proposed HTSS includes a linear formulation for valve loading effect, fuel cost, emission function, fuel constraint, and multi-performance power-discharge curves of hydro units as well as units' minimum up/down time. A GENCO can use the proposed methodology in their day-ahead scheduling to find the optimal decision for the UC for the next day. The new contributions of this paper with respect to the previous works can be briefly summarized as follows:

a) A new multiobjective model for the HTSS is proposed considering emissions in addition to cost function using linearized formulations. A new approach incorporating the lexicographic optimization and ε-constraint method is proposed to solve the multiobjective problem.

b) Different operating constraints of thermal and hydro units have been included in the proposed formulations. Also, all the nonlinear terms of the HTSS formulations have been converted to linear forms using mixed integer techniques and piece-wise linearization.

c) The generating units' contingencies and price uncertainty are explicitly considered in the stochastic programming of the HTSS problem using the roulette wheel mechanism and Lattice Monte-Carlo Simulation (LMCS).

d) Some discussions regarding emission trade, as a new paradigm in new era of power system operation, have been presented in the paper.

The remainder of this paper is organized as follows: In section II, the proposed stochastic modeling of HTSS problem is formulated concerning system's uncertainties. In section III, the MIP formulation for the stochastic multiobjective HTSS has been presented. Solution approach of the multiobjective optimization problem is discussed in section IV. In the next section, the IEEE 118-bus test system is studied to demonstrate effectiveness of the proposed scheme. Some relevant conclusions are drawn in the section VI.

II. Stochastic Modeling of Uncertainties

There are some uncertain factors like market price and outages of generating units that affect the profit of the GENCO. However, several methods exist to characterize the uncertainty of the problem due to market price and outages of generating units, among which Monte-Carlo Simulation (MCS), time series technique, input/output hidden Markov model and Generalized Auto-Regressive Conditional Heteroskedasticity (GARCH) model are the well-known ones. However, this paper uses the Lattice Monte-Carlo Simulation (LMCS) method to consider the outages of generating units as well as the price uncertainty based on the price forecast error. Lattice rule is an algorithm to generate low-discrepancy procedures leading to better results than ordinary MCS method [16]. An *n*-point lattice rule of rank-*r* in *d*-dimension is defined as follows [16]:

$$\sum_{l=1}^{r} \frac{k_l}{n_l}.v_l \bmod 1 \quad k_l = 0,1,...,n_l - 1 \;\; l = 1,...,r \tag{1}$$

where, $v_1, v_2, ...$ and v_r are randomly generated and linearly independent *d*-vector of integers. The dimension *d* indicates the number of random values required to generate each scenario and n_l represents the

variation range of k_l in rank l (l= 1,2, …, r). The points generated by the rank-1 lattice rule and ordinary MCS are shown in Fig. 1(A) and 1(B), respectively. The points generated by the LMCS have a much more uniform distribution and better covers the space of the figure. Therefore, the LMCS is implemented based on the Forced Outage Rate (FOR) of units to model generating units' uncertainties. Fig. 2 shows a typical continuous distribution function of the price forecast error along with its discretization. Here, seven intervals are centered on the zero mean and each of the intervals is one price forecast error standard deviation (σ) wide, as done in [28]. On the basis of different price forecast levels and their obtained probabilities from the PDF, roulette wheel mechanism [29-30] is implemented to generate price scenarios for each hour. For this purpose, at first, the probabilities of different price forecast levels are normalized such that their summation becomes equal to unity. Then the range of [0, 1] is accumulated by the normalized probabilities as shown in Fig. 3. After that, random numbers are generated between [0, 1]. Each random number falls in the normalized probability range of a price forecast level in the roulette wheel. That price forecast level is selected by the roulette wheel mechanism for each hour of a scenario.

Scenario reduction techniques can be ultimately employed to reduce the number of scenarios while maintaining a good approximation of the system uncertain behavior. In this paper, the basic idea of the scenario reduction is to eliminate a scenario with very low probability and scenarios that are very similar [28-29]. Accordingly, the scenarios with higher probabilities as well as dissimilar ones should be extracted (NS scenarios) to be implemented in the stochastic multiobjective HTSS problem. The probability of each generated scenario can be calculated as follows:

$$\mathrm{P}(s)=\prod_{t\in T}\left\{\sum_{k=1}^{NP}\left(W^{P}_{k,t,s}.\alpha_k\right)\left(\prod_{i\in I}W_{i,t,s}(1-FOR(i))+(1-W_{i,t,s})FOR(i)\right)\left(\prod_{j\in J}W_{j,t,s}(1-FOR(j))+(1-W_{j,t,s})FOR(j)\right)\right\} \quad (2)$$

where, $\sum_{k=1}^{NL}W^{P}_{k,t,s}=1$.

The binary parameters $W^{P}_{k,t,s}$, are determined by the roulette wheel mechanism and $W_{i,t,s}$ and $W_{j,t,s}$are specified by the LMCS for each hour of each scenario. Subsequently, the normalized probability of scenarios can be calculated as follows:

$$\mathrm{Pr}(s)=\frac{\mathrm{P}(s)}{\sum_{s=1}^{NS}\mathrm{P}(s)} \quad (3)$$

The flowchart of the proposed scenario-based stochastic modeling of uncertainties is illustrated in Fig. 4.

The idea of the stochastic programming of the HTSS problem is to construct or sample possible options for uncertain circumstances, solve the deterministic optimization problem for the possible options, and select a good combination of the outcomes to represent the stochastic solution. So, in the proposed stochastic HTSS structure, the expected value is considered, which is the aggregation approach adopted in many stochastic frameworks such as [16]. It is noted that theoretically deviation from the minimum limits constraints, such as (18) of the paper, might occur in the aggregated solution obtained by the expected value operator. For a better illustration of this matter, simply consider two scenarios with the equal probability wherein a unit is assigned ON and OFF states in these two, respectively. Aggregated value of the generation output of this unit obtained by the expected value operator is half of its generation in the ON scenario, which may deviate from its minimum limit. On the other hand, deviation from the maximum limit constraints, such as (18) of the paper, cannot be occurred in the expected value based scenario aggregation result, since each scenario result separately satisfy the maximum limit constraints and so a weighted average of the scenario results cannot deviate from these constraints. At the same time, we observed no deviation from the minimum limit constraints in our all experimental results, since our remained scenarios after scenario reduction do not have much diversity (the low probability scenarios are removed by the scenario reduction technique). So, deviation from the minimum limit constraints by the expected values is not observed in our results. However, if in a test case, deviation from these constraints is likely to be occurred then inter-scenario constraints can be used to avoid such deviations. For instance, in [16], bundle constraints are proposed to avoid infeasible solutions with the expected value based scenario aggregation. Another alternative is to impose these constraints on the aggregated results (expected values). However, both approaches lead to inter-scenario constraints and so the obtained problem becomes more complex than the present stochastic framework, which can be solved using decomposition techniques (e.g., benders decomposition). This matter is beyond the scope of this paper and will be considered in our future work.

III. MIP Formulation for the stochastic multiobjective HTSS

The proposed multiobjective stochastic framework for HTSS contains two objective functions as follows:

$$\text{Objective Functions} = \begin{cases} F_1 & \text{expected profit maximization} \\ F_2 & \text{expected emmision minimization} \end{cases} \tag{4}$$

Where F_1, and F_2 are the objective functions of the HTSS as following subsections.

III.A. Expected Profit Maximization

The main objective function of problem is the Expected Profit (*EP*) maximization, written as follows:

$$F_1 : \max EP = \pi^b(t)p^b(t) + \sum_{s \in NS} \Pr(s)\, PROFIT(s) \tag{5}$$

$$PROFIT(s) = \sum_{t \in T} \left\{ \begin{array}{l} \pi^{sp}(t,s)p^{sp}(t,s) + \\ \sum_{i \in I} \left\{ \pi^{sr}(t,s)R(i,t,s) + \pi^{ns}(t,s) \begin{pmatrix} N_u(i,t,s) \\ +N_d(i,t,s) \end{pmatrix} \right\} \\ +\sum_{j \in J} \left\{ \pi^{sr}(t)R(j,t,s) + \pi^{ns}(t,s) \begin{pmatrix} N_u(j,t,s) \\ +N_d(j,t,s) \end{pmatrix} \right\} \\ -\sum_{i \in I} \{F(i,t,s) + A_i z(i,t,s) + B(i,t,s) + C(i,t,s)\} \\ -\sum_{j \in J} A_j y(j,t,s) \end{array} \right\} \tag{6}$$

where, the *EP* is the main objective function which equals to constant revenue from bilateral contract (the first term of (5)) plus the summation of revenue of each scenario times to its corresponding probability (the second term of (5)). Equation (6) shows the profit of each scenario and the first term of this equation is related to revenue from the sales of energy. Second and third term refer to revenue from the sales of ancillary services on the spot market by thermal and hydro units, respectively. Fourth and 5th terms stand for thermal and hydro units cost, respectively. Subsection III.C shows more details for thermal units cost which consists of fuel cost, shut-down cost, start-up cost and valve loading effects cost, respectively. The last term of equation (6) refers to hydro plants start-up cost because of wear and tear of the windings and mechanical equipments, loss of water during maintenance and start-up and finally malfunctions in the control equipments [31].

III.B Expected Emission Minimization

The second objective function of the HTSS problem is to minimize the expected emission of thermal units which can be written as follows:

$$F_2 : \min EE = \sum_{s \in NS} \Pr(s) \sum_{i \in EGR} \sum_{t \in T} \left\{ E_{\min}(i) I_d(i,t,s) + \sum_{n=1}^{NE} \begin{pmatrix} \beta_n(i,t,s) E(p_{n-1}^u(i)) \\ +be_n(i)\delta_n(i,t,s) \end{pmatrix} + SUE(i)y(i,t,s) + SDE(i)z(i,t,s) \right\} \tag{7}$$

Where, EGR={SO_2 , NO_x}, since theSO_2 and NO_x are the most important emissions in power generation industry which have harmful effects on the environment [32]. The emission function is linearized using the piecewise linear

approximation as shown in Fig. 5. In order to more accurately model the problem, the emission function consists of emission due to start-up and shut-down of thermal units. Note that the first term represents the emission caused by off thermal units when providing non-spinning reserve [13].

The proposed HTSS framework is subject to the equality and inequality constraints. One of them is that the total generated power of thermal and hydro units should be equal to the total power sold in the spot market and bilateral contract for each hour of each scenario as follows:

$$\sum_{i\in I} p(i,t,s) + \sum_{j\in J} p(j,t,s) = p^{b}(t) + p^{sp}(t,s);\ \ \forall t \in T, \forall s \in S \tag{8}$$

The other constraints of the thermal units and hydro units are presented in the subsection III. C and D, respectively.

III.C Thermal units' model

This subsection pertains to the linearization of all the nonlinear equations of the thermal units.

A. Fuel cost function considering POZ

Usually quadratic function is used to present the fuel cost of the thermal units. However, thermal units cannot operate in some specific zones due to the physical operating restrictions. Consequently, their fuel cost function is a discrete function. The proposed piecewise linear model for fuel cost function with *M* POZs is as follows as:

$\forall i \in I, \forall t \in T, \forall s \in S$

$$F(i,t,s) = \sum_{n=1}^{M+1} \left[\beta_n(i,t,s) F(p^{u}_{n-1}(i)) + b_n(i)\delta_n(i,t,s) \right] \tag{9}$$

$$P(i,t,s) = \sum_{n=1}^{M+1} [\, p^{u}_{n-1}(i)\beta_n(i,t,s) + \delta_n(i,t,s)] \tag{10}$$

where, $F(i,t,s)$ is the piecewise linearized fuel cost function and $\beta_n(i,t,s)$ is binary variable and equal to 1 if power block *n* for thermal unit *i* of piecewise fuel cost curve selected. The second term in equation (9) is related to the slope and generation of power block *n*. The amount of unit output is determined by (10). The other constraints for linearization of fuel cost function can be formulated as follows [33]: $\forall i \in I, \forall t \in T, \forall s \in S$

$$\delta_n(i,t,s) \geq 0\,;\ n = 1,2,...,M+1 \tag{11}$$

$$\delta_n(i,t,s) \leq [\, p^{d}_{n}(i) - p^{u}_{n-1}(i)]\beta_n(i,t,s);\ \ n = 1,2,...,M+1 \tag{12}$$

$$\sum_{n=1}^{M+1} \beta_n(i,t,s) = I(i,t,s) \tag{13}$$

where, $p_0^u(i) = p_{\min}(i)$ and $p_{M+1}^d(i) = p_{\max}(i)$ in (12). Equation (11) indicates that power output of each block is positive Equation (12) shows he generated power of each unit is restricted by its upper limit. Constraint (13) forces the selected thermal unit to operate only at one of the operating zones.

B. Valve loading effect cost

The valve loading effect is modeled as an absolute sinus function of the generated power [19-21] which has a nonlinear form. In the proposed MIP formulation for the HTSS problem, the valve loading effect is linearized, as shown in Fig. 6, according to the following equations.

$$C(i,t,s) = \frac{2e_i f_i}{\pi}\left\{\sqrt{2}\sum_{n=0}^{k_i}[\psi_{4n+1}(i,t,s) - \psi_{4n+4}(i,t,s)] + (2-\sqrt{2})\sum_{n=0}^{k_i}[\psi_{4n+2}(i,t,s) - \psi_{4n+3}(i,t,s)]\right\} \quad \forall i \in I, \forall t \in T, \forall s \in S \tag{14}$$

$$p(i,t,s) = p_{\min}(i) I(i,t,s) + \sum_{n=0}^{k_i}[\psi_{4n+1}(i,t,s) + \psi_{4n+2}(i,t,s) + \psi_{4n+3}(i,t,s) + \psi_{4n+4}(i,t,s)] \quad \forall i \in I, \forall t \in T, \forall s \in S \tag{15}$$

$$\frac{\pi}{4f_i}\chi_1(i,t,s) \le \psi_1(i,t,s) \le \frac{\pi}{4f_i} I(i,t,s) \quad \forall i \in I, \forall t \in T, \forall s \in S \tag{16}$$

$$\frac{\pi}{4f_i}\chi_n(i,t,s) \le \psi_n(i,t,s) \le \frac{\pi}{4f_i}\chi_{n-1}(i,t,s); \qquad \forall i \in I, \forall t \in T, n = 2,3,...,x_i, \forall s \in S \tag{17}$$

$$k_i = ceil[f_i \frac{p_{\max}(i) - p_{\min}(i)}{\pi}], \quad x_i = ceil[4f_i \frac{p_{\max}(i) - p_{\min}(i)}{\pi}]$$

The *ceil* (.) function, approximate its argument to its nearest upper integer value. For instance *ceil* (3.1)=4.

where, e_i and f_i are coefficients of valve point effects for *i*th thermal unit and $\psi_n(i,t,s)$ is power generated by *n*th block. Eq. (15) indicates that the generated power by the thermal unit *i* at the hour *t* of scenario *s* is the sum of its minimum power output when that unit is committed, plus the produced power in each block. Constraint (16) determines the thermal unit output in the first block. In other words, the thermal units output in the first block should smaller than or equal to π/4fi. In (16), the binary variable $I(i,t,s)$ prevents unit *i* to generate power, if it is decommitted at the hour *t* of the scenario *s*. In order to restrict the produced power in each block, the binary variable $\chi_n(i,t,s)$ is introduced in constraints (16) and (17). In fact, the binary variable will be equal to 1, if the output of the

thermal unit i at the hour t of the scenario s is more than the upper limit of the block n. In other words, the binary variable $\chi_n(i,t,s)=1$ if $p(i,t,s) > P_{\min}(i,t,s) + \frac{n\pi}{4f_i}$.

C. Capacity limits of thermal units

The upper and lower limit constraints of the thermal units including the ramp up limit (RUL) and ramp down limit (RDL) can be written as follows:

$$p_{\min}(i)I(i,t,s) \le p(i,t,s) \le \bar{p}(i,t,s) \tag{18}$$

$$\bar{p}(i,t,s) \le p_{\max}(i)\{I(i,t,s) - z(i,t+1,s)\} + SD(i)Z(i,t+1,s) \tag{19}$$

$$p(i,t-1,s) - p(i,t,s) \le SD(i)Z(i,t,s) + RDL(p(i,t,s)) \tag{20}$$

$$p(i,t+1,s) - p(i,t,s) \le SU(i)y(i,t+1,s) + RUL(p(i,t,s)) \tag{21}$$

Equation (18) indicates the power generation limit of thermal units and equation (19) illustrates the upper limit of power generation by thermal units at each time. The shut-down ramp rate and Ramp-Down Limit (RUL) are shown in equation (17) while equation (18) indicates the start-up ramp rate and Ramp-Up Limit (RUL).

D. Dynamic RDL and RUL

Based on the work [22], the proposed dynamic ramp rate of the thermal units is as follows:

$$RDL(p(i,t,s)) = \sum_{n=1}^{M+1} RDL_n(i)\beta_n(i,t,s) \quad \forall i \in I, \forall t \in T, \forall s \in S \tag{22}$$

$$RUL(p(i,t,s)) = \sum_{n=1}^{M+1} RUL_n(i)\beta_n(i,t,s) \quad \forall i \in I, \forall t \in T, \forall s \in S \tag{23}$$

According to (22) and (23), the dynamic ramp rate is related to thermal units by $\beta_n(i,t,s)$.

E. Other constrains of thermal units

Reserve Services: In order to sustain sudden events of power systems such as the outages of transmission lines and generators, the operating services (spinning reserve and non-spinning reserve) are considered as done by [16]. The other constraints of the proposed HTSS problem, as addressed in [2, 34], are: time varying start-up cost function, Minimum Up-Time (MUT) and Minimum Down-Time (MDT), and Logical status of commitment. Also, the fuel limit constraints are taken from [7, 16].

III.D. Hydro units' model

In this section the constraints of the hydro units are addressed.

A. Linear formulations for volume and multi-performance curves

The linear formulations of the hydro units with L performance curves, as shown in Fig. 7, are as the following equations:

$$v(j,t,s) \geq v_0(j);\ \forall j \in J \tag{24}$$

$$v(j,t,s) \leq v_L(j)\beta_{L-1}(j,t,s) + \sum_{n=2}^{L} v_{n-1}(j)[\beta_{n-2}(j,t,s) - \beta_{n-1}(j,t,s)] \tag{25}$$

$$v(j,t,s) \geq v_{L-1}(j)\beta_{L-1}(j,t,s) + \sum_{n=3}^{L} v_{n-2}(j)[\beta_{n-2}(j,t,s) - \beta_{n-1}(j,t,s)] \tag{26}$$

$$\beta_1(j,t,s) \geq \beta_2(j,t,s) \geq .... \geq \beta_{L-1}(j,t,s) \tag{27}$$

Equation (24) indicates that the volume of each hydro plant at each period should be greater than the minimum content of that hydro plant. Equations (25) and (26) stand for the right head corresponding to volume. The equations (24) to (27) determine the integer variable of $\beta_n(j,t,s)$ for performance curves based on the water volume. In other words, these equations choose the right curve for head according to the content level.

B. Linear power-discharge performance curves

The linear relationship between generated powers, discharged water and performance curves is presented as:

$$p(j,t,s) - \underline{p}_k(j)I(j,t,s) - \sum_{n\in N} q_n(j,t,s)b_n^k(j) - \bar{p}(j)[(k-1) - \sum_{n=1}^{k-1}\beta_n(j,t,s) + \sum_{n=k}^{L-1}\beta_n(j,t,s)] \leq 0 \quad ,1 \leq k \leq L \tag{28}$$

$$p(j,t,s) - \underline{p}_k(j)I(j,t,s) - \sum_{n\in N} q_n(j,t,s)b_n^k(j) + \bar{p}(j)[(k-1) - \sum_{n=1}^{k-1}\beta_n(j,t,s) + \sum_{n=k}^{L-1}\beta_n(j,t,s)] \geq 0 \quad ,1 \leq k \leq L \tag{29}$$

In above constraints, $p(j,t,s)$ is power generated by hydro plant at hour t and scenario s and $\underline{p}_k(j)$ is minimum generation of kth head. Proper head appointed by $\beta_n(j,t,s)$ and $\bar{p}(j)$ is capacity of hydro plant j and $q_n(j,t,s)$ is water discharge of block n and $b_n^k(j)$ is slope of the block n of the performance curve k of hydro plant j.

C. The other constraints of hydro units

The water discharge limits are similar to those presented in [23]; however, in the proposed stochastic multiobjective HTSS model the spillage effect is also considered [2]. Also, the initial value of the reservoir, water balance [2], [23], and operating services [16] are considered in the proposed HTSS problem.

IV. Multiobjective Mathematical Programming (MMP)

In Multiobjective Mathematical Programming (MMP), there is more than one objective function and there is no single optimal solution that simultaneously optimizes all the objective functions. A well-organized technique to solve MMP problems owning one main objective function among all objective functions is the ε-constraint method which is used to solve the proposed stochastic multiobjective HTSS problem in this paper. In general, the *ε*-constraint technique [35-36] optimizes the main objective function f_1 considering the other objective functions as constraints:

$$\begin{aligned} &\min f_1(\bar{x}) \\ &\textit{subject to} \quad f_2(\bar{x}) \le e_2 \quad f_3(\bar{x}) \le e_3 \quad \ldots \quad f_p(\bar{x}) \le e_p \end{aligned} \tag{30}$$

where, the subscript p indicates the number of competing objectives functions of the MMP problem and $\bar{x}$ refers to the vector of decision variables. In (30), it is assumed that all p objective functions should be minimized. In order to properly apply the *ε*-constraint method, the ranges of at least p-1 objective functions are needed that will be used as the additional objective function constraints. The most common approach is to calculate these ranges from the payoff table. To calculate the payoff table for a MMP problem with p competing objective functions, at first, the individual optima of the objective functions f_i are calculated. The optimum value of f_i is indicated by $f_i^*(\bar{x}_i^*)$ where $\bar{x}_i^*$ refers to the vector of decision variables which optimizes the objective function f_i. Then, with the solution that optimizes the objective function f_i, the value of the other objective functions $f_1, f_2, \ldots, f_{i-1}, f_{i+1}, \ldots, f_p$ is calculated, which are represented by $f_1(\bar{x}_i^*), f_2(\bar{x}_i^*), \ldots, f_{i-1}(\bar{x}_i^*), f_{i+1}(\bar{x}_i^*), \ldots, f_p(\bar{x}_i^*)$. The i^{th} row of the payoff table includes $f_1(\bar{x}_i^*), f_2(\bar{x}_i^*), \ldots, f_i^*(\bar{x}_i^*), \ldots, f_p(\bar{x}_i^*)$. In this way all rows of the payoff table are calculated as follows:

$$\Phi = \begin{pmatrix} f_1^*(\bar{x}_1^*) & \cdots & f_i(\bar{x}_1^*) & \cdots & f_p(\bar{x}_1^*) \\ \vdots & \ddots & & & \vdots \\ f_1(\bar{x}_i^*) & \cdots & f_i^*(\bar{x}_i^*) & \cdots & f_p(\bar{x}_i^*) \\ \vdots & & & \ddots & \vdots \\ f_1(\bar{x}_p^*) & \cdots & f_i(\bar{x}_p^*) & \cdots & f_p^*(\bar{x}_p^*) \end{pmatrix} \tag{31}$$

The payoff table has p rows and columns. The j^{th} column of the payoff table includes the obtained values for the objective function f_j among which the minimum and maximum values indicate the range of the objective function f_j for the ε-constraint method. To enhance the ε-constraint method to the proposed MMP solution technique, at first a few concepts should be introduced. Without losing generality, it is again supposed that all objective functions should be minimized.

Utopia point is a specific point, generally outside of the feasible region, that corresponds to all objectives simultaneously being at their best possible values. The utopia is written as:

$$f^U = \left[f_1^U, ..., f_i^U, ..., f_p^U \right] = \left[f_1^*(\bar{x}_1^*), ..., f_i^*(\bar{x}_i^*), ..., f_p^*(\bar{x}_p^*) \right] \tag{32}$$

Nadir point is a point in the objective space where all objective functions are simultaneously at their worst values. The nadir point is written as:

$$f^N = \left[f_1^N, ..., f_i^N, ..., f_p^N \right] \tag{33}$$

Where:

$$f_i^N = \max_{\bar{x}} f_i(\bar{x}), \qquad \text{subject to} \quad \bar{x} \in \Omega \tag{34}$$

Where, Ω represents the feasible region. A close concept to nadir point is pseudo nadir point defined as follows:

$$f^{SN} = \left[f_1^{SN}, ..., f_i^{SN}, ..., f_p^{SN} \right] \tag{35}$$

$$f_i^{SN} = \max \left\{ f_i(\bar{x}_1^*), ..., f_i^*(\bar{x}_i^*), ..., f_i(\bar{x}_p^*) \right\} \tag{36}$$

It is noted that utopia, nadir and pseudo nadir points are defined in the objective space, which is a vector space with the objective functions as its dimensions. In the ε-constraint technique, the range of each objective function in the payoff table is determined based on the utopia and pseudo nadir points, that is:

$$f_i^U \le f_i(\bar{x}) \le f_i^{SN} \tag{37}$$

Optimization of MMP problems is to identify the set of Pareto optimal solutions. For a general multi-objective optimization problem of (25), a point $\bar{x}^* \in \Omega$ is Pareto optimal or efficient solution for the MMP problem if and only if there is no $\bar{x} \in \Omega$ such that $f_i(\bar{x}) \le f_i(\bar{x}^*)$ for all i=1, 2, ... ,p with at least one strict inequality.

After finding the range of all objective functions based on (37), the ε-constraint technique divides the range of p-1 objective functions $f_2, \ldots, f_p$ to $q_2, \ldots, q_p$ equal intervals using $(q_2\text{-}1), \ldots, (q_p\text{-}1)$ intermediate equidistant grid points, respectively. Considering the minimum and maximum values of the range, we have in total $(q_2+1), \ldots, (q_p+1)$ grid points for $f_2, \ldots, f_p$, respectively. So, we should solve $\prod_{i=2}^{p}(q_i+1)$ optimization subproblems, where the subproblem $(n2, \ldots, np)$ has the following form:

$$\begin{aligned} &\min f_1(\bar{x}) \\ &\textit{subject to} \quad f_2(\bar{x}) \le e_{2,n2}, \quad \cdots, \quad f_p(\bar{x}) \le e_{p,np} \end{aligned} \tag{38}$$

$$e_{2,n2} = f_2^{SN} - \left(\frac{f_2^{SN} - f_2^{U}}{q_2} \right) \times n2 \qquad n2 = 0,1,\ldots,q_2 \tag{39}$$

$$e_{2,np} = f_p^{SN} - \left(\frac{f_p^{SN} - f_p^{U}}{q_p} \right) \times np \qquad np = 0,1,\ldots,q_p \tag{40}$$

where, the superscript U and SN refer to the value of the objective function in the utopia and pseudo nadir points as shown in (32) and (36), respectively. The constraints of the MMP problem should be also considered in each of these optimization subproblems in addition to the objective function constraints mentioned in (38). By solving each optimization subproblem, one Pareto-optimal solution is obtained in the ε-constraint technique. Some of these optimization subproblems may have infeasible solution space, which will be discarded. Among the obtained Pareto-optimal solutions, the most preferred one is selected by the decision maker.

The advantages of the proposed method can be listed as following:

i. For linear problems, the weighting method generates only efficient extreme solutions. On the contrary, the epsilon-constraint method is able to produce non-extreme efficient solutions [35].

ii. Despite the weighting method, the epsilon-constraint method can produce unsupported efficient solutions in multiobjective integer and mixed integer programming problems [35].

iii. In the epsilon-constrained method, the scaling of the objective functions is not necessary while this is needed in the weighting method [35].

iv. In the epsilon-constraint method, the number of the generated efficient solutions can be controlled by properly adjusting the number of grid points in each one of the objective function ranges [35].

Despite the above advantages, the epsilon-constraint method has two points that need attention:

i. Firstly, the range of the objective functions over the efficient set is not optimized. To solve this problem, lexicographic optimization technique is proposed here.

ii. Secondly, the generated Pareto optimal solutions by the epsilon-constraint method may be dominated or inefficient solutions. Augmented-weighted epsilon-constraint technique is suggested to remedy this deficiency. The details of incorporating lexicographic optimization and augmented-weighted epsilon-constraint technique have been described in our previous paper in the area [37, 38]. To avoid tautology in writing, these matters have not been repeated in this paper.

The presented MMP solution method is formed by coming together the augmented-weighted ε-constraint technique and lexicographic optimization. The procedure of the proposed method can be stated as follows:

Step 1: By employing the lexicographic optimization approach, the payoff table pertaining to a MMP problem is computed.

Step 2: The range of the ith objective function (i = 2, 3,.., p) is determined using payoff table.

Step 3: According to formulation proposed in (39-40), the range of at least p-1 objective functions is divided into qi (i = 2, 3,.., p) equal intervals.

Step 4: The feasible optimization sub-problems in (38) are solved applying the presented MMP solution method to produce the Pareto efficient solution while the infeasible ones are discarded.

Step 5: The efficient solutions derived through step 4 is evaluated using the Fuzzy decision making process; Eq. (41-43), to choose the most desired Pareto optimal solution.

The proposed optimization framework for ε-constraint optimization method for MMP problem is illustrated in Fig. 8.

A. Fuzzy decision maker

In order to choose the best compromise solution among the obtained Pareto optimal solutions by the ε-constraint method, a fuzzy decision maker is proposed which can softly select the most preferred compromise solution among the Pareto solutions [29, 37-42].For this purpose, the fuzzy decision maker calculates a linear membership function for each objective function in each Pareto optimal solution, which measures the relative distance between the value

of the objective function in the Pareto optimal solution from its values in the respective utopia and pseudo nadir points. The mathematical formulation of these membership functions for the MMP market clearing problem is as follows:

$$\mu_{n=1}^{r}=\begin{cases}0 & f_n^r \le f_n^{SN}\\ \dfrac{f_n^r-f_n^{SN}}{f_n^U-f_n^{SN}} & f_n^{SN}\le f_n^r\le f_n^U \quad \text{(Maximization)}\\ 1 & f_n^r \ge f_n^U\end{cases} \tag{41}$$

$$\mu_{n=2}^{r}=\begin{cases}1 & f_n^r \le f_n^U\\ \dfrac{f_n^{SN}-f_n^r}{f_n^{SN}-f_n^U} & f_n^U\le f_n^r\le f_n^{SN} \quad \text{(Minimization)}\\ 0 & f_n^r \ge f_n^{SN}\end{cases} \tag{42}$$

The fuzzification process described in (41) and (42) is used for the objective functions that should be maximized and minimized, respectively. The total membership function (total degree of optimality) of each Pareto optimal solution is computed considering the individual membership functions and the relative importance of the objective functions (w_n values) as follows:

$$\mu^r=\frac{\sum_{n=1}^{p} w_n.\mu_n^r}{\sum_{n=1}^{p} w_n} \tag{43}$$

The most preferred solution refers to the Pareto solution with the highest value of μ^r or the highest preference for the MMP problem. This solution more optimizes the objective functions of the MMP problem, considering their relative importance, than the other Pareto solutions [29, 37-42].

B. Emission trade

In some circumstances, selling the emission quota is more profitable than selling the power; therefore, the GENCO can use this opportunity to obtain more profit. On the other hand, in some cases, the GENCO is forced to procure emission quota, to increase its output to obtain more profit. The total profit of the GENCO considering emission arbitrage is as follows:

$$EA = EP + \pi^E \times \left(E^{QUATA} - EE\right) \tag{44}$$

where *EA,* denotes that GENCO's total profit in dollars, *EP* is the obtained profit of each Pareto optimal solution in dollars, $\pi^E$is the price of emission in $/lbs, E^{QUOTA} is the emission quota in (lbs) and finally *EE* is the expected generated emission of each Pareto optimal solution in (lbs). If $E^{QUOTA}>EE$, then an excess quota is available that can be sold in the market. On the other hand if $E^{QUOTA}<EE$ then the GENCO need to purchase additional emission quota [52]. Hence, for each Pareto-optimal solution *EA* is calculated and then the solution with the highest value of *EA* can be chosen as the best solution by the GENCO.

V. Case Study

The case study used to illustrate the proposed stochastic multiobjective HTSS is the well-known IEEE 118-bus test system. This system contains 54 thermal units which are10 oil-fired, 11 gas-fired and 33 coal-fired units. Eight hydro units are considered that their required data are taken from [23]. The POZ data and valve loading coefficients are taken from [43]. Based on [2], the start-up cost of thermal units is linearized in 3 blocks. Also, based on [32] the emission functions of SO_2 and NO_x have been linearized in 4 blocks as shown in Fig. 5. It is assumed that both $SU(i)$ and $SD(i)$ are equal to $0.7*P_{max}(i)$.Bilateral contract at each hour is 1000 MWh at the price of 40$/MWh. Also, it is assumed that the forecasted water inflow to the hydro plants is deterministic value while the proposed scheduling problem is considered for the short-term horizon plan. Due to lack of data, without the loss of generality, fix ramp rate data is used. For hydro units, 3 performance curves are used that each of them is linearized in 4 blocks as shown in Fig. 7. Total spinning and non-spinning reserves which can be sold at each hour of each scenario is 500MW. Other data for thermal units are taken from [43]. Thermal units 5, 10, 11, 28, 36, 43, 44 and 45 have valve loading effect cost and thermal units 7, 10, 30, 34, 35 and 47 have POZs limitations.

The proposed MIP optimization problem of the stochastic multiobjective HTSS has been modeled in GAMS [44] software using CPLEX solver on a personal computer Pentium IV, 2.4 GHz with 2 GB RAM. The optimization problem includes millions of continuous and discrete variables which increase the solution time and computational burden. For this reason, without the loss of generality, in the case study of the proposed stochastic multiobjective HTSS framework, the number of scenarios and also the periods of time scheduling (hours) are reduced. However, the parallel computation method and decomposing approach can significantly decrease solution time of the HTSS optimization problem. According to this study, the number of scenarios after scenario reduction is reduced to 10.

Also, 10 periods (hours) are considered for the stochastic multiobjective HTSS. In other words in each scenario, the system is scheduled over ten successive hours. Accordingly, the case study of the stochastic multiobjective HTSS includes one deterministic (non-contingent generating units and without price forecast error) scenario plus nine scenarios considering the generating units' contingencies as well as the price forecast errors. In this study, five different price forecast levels are considered as shown in Fig. 2 and the MCP for each hour of each scenario (except the first scenario that is deterministic) is determined based on the roulette wheel mechanism described in the section II.

The ε-constraint is used to find the Pareto solutions of the stochastic multiobjective HTSS problem. In the ε-constraint method, F_1 (expected profit maximization) is considered as the main objective function. To solve the MMP problem, 19 grid points (q_2=19) for F_2, i.e. *EE*, is used for obtaining Pareto optimal solutions. So, the problem should be solved totally (q_2+1 = 20) times to obtain the Pareto optimal solutions of the stochastic multiobjective HTSS which all of them have feasible solution.

In order to better explanation of the proposed framework, four cases are considered which are:

Case 1-*Deterministic single objective HTSS*: In case 1, the objective function is the profit maximization and include only one scenario wherein it is assumed that all units can be on if necessary after solving optimization problem and forecasted price is equal to the actual price. Therefore this case include equations of (5), (6), and (8) to (29).

Case 2-*Stochastic single objective HTSS*: In this case, the objective function is profit maximization including uncertainty of price and availability of generation units. Therefore this case includes equations (1)-(6), (8)-(29), and (45)-(46).

Case 3-*Deterministic multiobjective HTSS*: The objective functions of this case are profit maximization and emission minimization. Also, it includes only one scenario wherein all units can be on if necessary after solving optimization problem and the forecasted price is equal to the actual price. Therefore, this case includes equations (4) to (44).

Case 4-*Stochastic multiobjective HTSS*: In case 4, the objective functions are profit maximization and emission minimization. Also, the uncertainty of price and availability of generation units has been considered in the formulation. Accordingly, this case includes equations of (1) to (46).

The results of cases 1 and 2 are shown in Table I. The expected profit of the stochastic HTSS is lower than the profit in deterministic HTSS for the reason that in the stochastic framework in each scenario, some efficient units may

decommitted based on their forced outage and therefore the profit of the GENCO is decreased. This difference in the profit can be interpreted as the value of *perfect information* [32]; i.e., the lack of information of the exact market price and also the exact status of generating units causes the GENCO to lose 6782 $ (2535224-2528442 = 6782$) of profits. Also, the amounts of the emissions are shown in Table I.

For deterministic multiobjective HTSS, only 5 of 20 Pareto optimal solutions are reported in Table II. The results show that the GENCO's emission is increased if the GENCO pursue more profit. In other words, obtaining more profit results in more emission showing the conflicting nature of these two objective functions. The best compromise solution can be selected by the fuzzy method or arbitrage approach [32], based on the GENCO's priority to obtain more profit or lower emissions. The arbitrage approach will be explained more in this section.

In the case 4, the stochastic multiobjective HTSS is studied for 10 scenarios and 10 successive hours. The payoff table results of the case 4 are shown in Table III.

According to the Table III, both minimum and maximum value of the expected profit is lower than those of the deterministic ones. The minimum value of the expected profit is 1894347.22 $ which is lower than the lowest value of the profit in the deterministic HTSS as shown in the second column of the last row of Table II, i.e. 1899232.71 $. Similarly the maximum value of the profit is 2533858.45 $ for the stochastic case against 2535646.92 $ for the deterministic multiobjective HTSS as shown in the second column of the first row in the Table II. The difference in the profits is due to the uncertainty of price forecasting and units' outage.

To choose the optimal solution among the Pareto solutions of the problem, a fuzzy decision maker is used. The weighting factors (showing the importance of the objective function) are considered the same for 2 objective functions in the fuzzy decision maker (w_1=w_2=1). Results of equal weighting factors for these two objective functions are shown in Table IV. The membership value indicates the degree of optimality. If equal weighting factors are considered for two objective functions, then the total membership is obtained 0.616 for 20 Pareto solutions which is not acceptably optimized. However, changing the weighting factors can simply direct the decision maker to its interested solution. Nevertheless, the GENCO is more desirous to profit rather than the emission concerns. Therefore, the proposed method is solve again with the profit and emission weighting factors of 3 and 1, respectively, which logically searching for a Pareto solution with high value of the profit membership and low value of the emission membership as shown in Table V. From the Table V it can be seen that the membership value of the profit remarkably has been improved from 0.653 in case of equal weighting factors to 0.970 in the case of different

weights. The profit value in the Table V is equal to 2514601.40 $; indeed it is very close to its ideal value reported in the Table III. On the other hand, the emission is increased as its membership is low. In other words, according to the Table V, the GENCO prefers to obtain more profit rather than emission decrease.

Since GENCOs are more desirous to increase profit rather than decrease emission, in the stochastic multiobjective HTSS problem, the optimal solution can be also obtained using arbitrage opportunity to gain more profit. Therefore, the emission arbitrage formulation (44) is calculated for all the Pareto optimal solutions obtained by the ε-constraint method and the optimal solution is ultimately selected. The advantage of the arbitrage trade compared to the fuzzy method is that the emission quota is implicitly considered and the chosen solution is more economic and realistic from GENCOs viewpoint. The Pareto solutions and their related emission trade are shown in Table VI. These arbitrage scenarios are calculated based on the E^{QUOTA}=100,000 lbs, with different prices of emission, i.e. π^{E}= 1, 2 and 3 $/lbs, which are shown in the last three columns of the Table VI. The negative value for emission indicates that GENCOs emission quota is not enough and it should accordingly purchase emission. In the Table VI, the optimal solutions for each price of emission are represented with the bold numbers superscripted with asterisk. By the proposed method, the GENCO can readily analyze arbitrage opportunities and make a decision that improves the total profit.

Finally, the number of variables and constraints and solution time for the four cases are presented in Table VII. From the Table VII, it takes 6186 seconds to find the Pareto optimal solutions of the case 4 of the problem. This is mainly for dimensionality issue which includes thousands of equations, continuous and discrete variables. Also from this table, one can see that the execution time of the problem is dramatically increased as the number of equations and variables of the problem increases.

It is noted that the methods used to solve pure integer and mixed integer programming problems require dramatically more mathematical computation than those for similarly sized pure linear programs [44]. Many relatively small integer programming models take enormous amounts of time to solve.

Moreover, when the memory is limited, the CPLEX solver will automatically make adjustments which may negatively impact the performance [44]. The MIP nature of our problem on one hand, and relatively large dimensions and memory limitations on the other hand, causes our HTSS optimization problem to take 6186 seconds to be solved and find the Pareto optimal solutions. Nevertheless, the parallel computation and decomposing

approach can significantly decrease this solution time. However, this paper pertains to present the comprehensive model for the stochastic multiobjective HTSS problem rather than computational viewpoints of the problem.

V.A Comparative analysis

We have used works [45] to [48] to compare the results of the proposed framework with them. It should be mentioned that the objective function of works [45] to [48] is the cost function. Also, in these works, emission function has been considered as another objective function of the optimization problem. All these works have used a heuristic approach to solve the problem. While the frameworks proposed in [45] to [48] are not completely same as the proposed scheme in this paper, i.e. multiobjective hydrothermal self-scheduling problem with objective functions of profit maximization and emission minimization, therefore we compare our proposed method with these references [45] to [48]. Accordingly, we have used their data, constraints and objective functions to show the performance of the proposed approach. Considering the above assumptions, the results of this case study are summarized in the tables VIII and IX which are taken from [48]. If we solve the same problem by the proposed method in this paper, the fuel cost is 40766.83($) and emission value is 18278.76 (lb). It can be seen from results that the proposed method can find better solution for fuel cost and emission in comparison with the results of [45] to [48]. Also, table X shows power generation of each thermal and hydro unit in each hour by solving the problem using the proposed method.

Besides, in table XI, we can see the solution time of each method. It is inferred from this table that the proposed algorithm in this paper has better efficiency from the calculation speed.

VI. Conclusions

This paper presents a stochastic multiobjective HTSS framework in the form of MIP optimization problem in which the valve loading effect cost, dynamic ramp rate, POZs, fuel limitation are modeled all in linear form. It also includes multi-performance curves for hydro units making the HTSS framework more realistic. With the proposed method, each GENCO can cope with the uncertainties of the HTSS problem, i.e. price forecast error and generating units' outage. Besides, each GENCO can compromise the conflicting objectives of the expected profit maximization in such a way that the GENCO's concerns about the emission are to some extent relieved. Furthermore, the stochastic approach leads to a more efficient utilization of generating units, allowing the GENCOs to estimate the

effects of units' contingencies and price uncertainty on the HTSS results. Covering the uncertainties by the proposed stochastic multiobjective HTSS, each GENCO can bid in the day-ahead market so as to gain profit as much as possible. Using the arbitrage approach make it possible for the GENCO to purchase its required emission or sell its emission quota to obtain more profit.

The research work under way to a) present a stochastic model with other scenario reduction techniques; b) consider financial risk associated with the market price uncertainty, and c) use accelerated benders decomposition to reduce computational burden.

VII. References

[1] Shahidehpour M, Yamin H, and Li Z. Market Operations in Electric Power Systems: Forecasting, Scheduling, and Risk Management. New York: IEEE-Wiley, 2002.

[2] Bisanovic S, Hajro M, and Dlakic M. Hydrothermal self-scheduling problem in a day-ahead electricity market. Elect. Power Syst. Res. 2008; 78 (9): 1579-1596.

[3] Farhat IA, and El-Hawary ME. Optimization methods applied for solving the short-term hydrothermal coordination problem. Elect. Power Syst. Res. 2009; 79 (9): 1308–1320.

[4] Catalão JPS, Pousinho HMI, Mendes VMF. Hydro energy systems management in Portugal: Profit-based evaluation of a mixed-integer nonlinear approach. Energy; 2011, 36 (1): 500-507.

[5] Pousinho HMI, Mendes, VMF, Catalão JPS.A risk-averse optimization model for trading wind energy in a market environment under uncertainty. Energy 2011; 36 (8): 4935-4942.

[6] Catalão JPS, Pousinho HMI, Contreras J. Optimal hydro scheduling and offering strategies considering price uncertainty and risk management. Energy 2012; 37 (1): 237-244

[7] Wu L, Shahidehpour M, and Li T. GENCO's risk-based maintenance outage scheduling. IEEE Trans. Power Syst. 2008; 23 (1): 127-136.

[8] Wu L, Shahidehpour M, and Li Z. GENCO's risk-constrained hydrothermal scheduling. IEEE Trans. Power Syst. 2008; 23 (4): 1847-1858.

[9] Aghaei J, Shayanfar HA, Amjady N. Joint market clearing in a stochastic framework considering power system security. Applied Energy 2009; 86 (9): 1675-1682.

[10] Partovi F, Nikzad M, Mozafari B, Ranjbar A.A stochastic security approach to energy and spinning reserve scheduling considering demand response program. Energy 2011; 36 (5): 3130-3137.

[11] Ruiz PA, Philbrick CR and Sauer PW. Modeling approaches for computational cost reduction in stochastic unit commitment formulations. IEEE Trans. Power Syst. 2010; 25 (1): 588-589.

[12] Tseng CL and Zhu W. Optimal self-scheduling and bidding strategy of a thermal unit subject to ramp constraints and price uncertainty. IET Gener. Transm. Distrib. 2010; 4 (2): 125–137.

[13] Aghaei J, Ahmadi A, ShayanfarHA ,Rabiee R. Mixed integer programming of generalized hydro-thermal self-scheduling of generating units. Electr. Eng. 2013; 95(2):109-125.

[14] Moghimi H, Ahmadi A , Aghaei A, Najafi M. Risk constrained self-scheduling of hydro/wind units for short term electricity markets considering intermittency and uncertainty .Rene. Sust. Energy Rev. 2012; 16:4734–4743.

[15] Moghimi H; Ahmadi A; Aghaei; Rabiee A. Stochastic Techno-Economic Operation of Power Systems in the Presence of Distributed Power Generation. Int. J. Electr. Power Energy 2013, 45 (1): 477–488.r Generation. Int. J. Electr. Power Energy 2013, 45 (1): 477–488.

[16] Wu L, Shahidehpour M, and Li T. Stochastic security-constrained unit commitment. IEEE Trans. Power Syst. 2007; 22 (2): 800-811.

[17] Shrestha GB, Kai S, and GoelL. An efficient stochastic self-scheduling technique for power producers in the deregulated power market. Elect. Power Syst. Res. 2004; 71 (1): 91-98.

[18] Li MW, Li YP, Huang GH. An interval-fuzzy two-stage stochastic programming model for planning carbon dioxide trading under uncertainty. Energy 2011; 36 (9): 5677-5689.

[19] Meng K, Wang HG, Dong ZY, and Wong KP. Quantum-inspired particle swarm optimization for valve-point economic load dispatch. IEEE Trans. Power Syst. 2010; 25 (1): 215-222.

[20] Amjady N, and Nasiri-Rad H. Non-convex economic dispatch with AC constraints by a new real coded genetic algorithm. IEEE Trans. Power Syst. 2009; 24 (3): 1489-1502.

[21] AlRashidi MR, and El-Hawary ME. Hybrid particle swarm optimization approach for solving the discrete OPF problem considering the valve loading effects. IEEE Trans. Power Syst. 2007; 22 (4): 2030-2038.

[22] Li T; and Shahidehpour M. Dynamic ramping in unit commitment. IEEE Trans. Power Syst. 2007; 22 (3): 1379-1381.

[23] Conejo AJ, Arroyo JM, Contreras J, and Villamor FA. Self- scheduling of a hydro producer in a pool-based electricity market. IEEE Trans. Power Syst. 2002; 17 (4): 1265-1272.

[24] Noruzi MR, Ahmadi A, Sharaf AM, Esmaeel Nezhad A. Short-term environmental/economic hydrothermal scheduling. Electr. Power Syst. Res. 2014, 116: 117-127.

[25] Ahmadi A, Aghaei J, and Shayanfar HA. Stochastic self-scheduling of hydro units in joint energy and reserves markets. 19th Iranian Conference on Electrical Engineering (ICEE), 2011: 1 – 5.

[26] Karami M, Shayanfar HA, Aghaei J and Ahmadi A. Mixed Integer Programming of Security-Constrained Daily Hydrothermal Generation Scheduling (SCDHGS). Scientia Iranica (Article in press).

[27] Ahmadi A, Charwand M, and Aghaei J. Risk-constrained optimal strategy for retailer forward contract portfolio. Int. J. Elec. Power Energy Syst. 2013. 53:704–713.

[28] Wu L, Shahidehpour M, and Li T. Cost of reliability analysis based on stochastic unit commitment. IEEE Trans. Power Syst. 2008; 23 (3): 1364-1374.

[29] Karami M, Shayanfar HA, Aghaei A, and Ahmadi A. Scenario-based security-constrained hydrothermal coordination with volatile wind power generation. Renew. Sust. Energy Rev. 2013; 28: 726–737.

[30] Damousis IG, Bakirtzis AG, and Dokopolous PS. A solution to the unit-commitment problem using integer coded genetic algorithm. IEEE Trans. Power Syst. 2003; 19 (1): 198–205.

[31] Aghaei J, Karami M, Muttaqi KM, Shayanfar HA, and Ahmadi A. MIP based stochastic security-constrained daily hydrothermal generation scheduling. IEEE Sys. J. 2013; 99: 1-14

[32] Vahidinasab V, and Jadid S. Stochastic multiobjective self-scheduling of a power producer in joint energy and reserves markets. Elect. Power Syst. Res. 2010; 80 (7): 760–769.

[33] Daneshi H, Choobbari AL, Shahidehpour M, and Li Z. Mixed integer programming method to solve security constrained unit commitment with restricted operating zone limits. IEEE Int. Con. on EIT 2008: 187-92.

[34] Arroyo JM, Conejo AJ. Optimal response of a thermal unit to an electricity spot market. IEEE Trans. Power Syst. 2000; 15 (3): 1098-1104.

[35] Mavrotas G. Effective implementation of the ε-constraint method in multiobjective mathematical programming problems modified augmented. Appl. Math. &Comp. 2009; 213 (2): 455-465.

[36] Esmaili M, Shayanfar HA, Amjady N. Multi-objective congestion management incorporating voltage and transient stabilities. Energy 2009; 34 (9): 1401-1412.

[37] Ahmadi A, Aghaei J, Shayanfar HA, and Rabiee A. Mixed integer programming of multiobjective hydro-thermal self-scheduling. Appl. Soft Comp 2012. 12(8): 2137–2146.

[38] Aghaei J, Amjady N, and Shayanfar HA. Multi-objective electricity market clearing considering dynamic security by lexicographic optimization and augmented epsilon constraint method, Appl. Soft Comp. 2011, 11 (4): 3846–3858.

[39] Norouzi MR, Ahmadi A, Esmaeel Nezhad A, and Ghaedi A. Mixed integer programming of multi-objective security-constrained hydro/thermal unit commitment. Renew. Sust. Energy Rev. 2014, 29: 912-923.

[40] Ahmadi A, Ahmadi MR, and Esmaeel-nezhad A. A lexicographic optimization and augmented ε-constraint technique for short term environmental/economic combined heat and power dispatch. Electr. Power Comp. Syst. 2014, 42(9): 945-958.

[41] Charwand M, Ahmadi A, Heidari A, and Esmaeel-nezhad A. Benders decomposition and normal boundary intersection method for multi-objective decision making framework for an electricity retailer in energy markets. IEEE Syst. J. 2014, 99: 1-10.

[42] Mavalizadeh H, Ahmadi A. Hybrid expansion planning considering security and emission by augmented epsilon-constraint method. Electr. Power Energy Syst. 2014, 61: 90-100

[43] http://motor.ece.iit.edu/data.

[44] Generalized Algebraic Modeling Systems (GAMS), [Online] Available: http://www.gams.com.

[45] Basu M. Interactive fuzzy satisfying method based on evolutionary programming technique for multiobjective short-term hydrothermal scheduling. Electr Power Syst Res, 2004, 69: 277–285.

[46] Mandal KK, Chakraborty N. Short-term combined economic emission scheduling of hydrothermal power systems with cascaded reservoirs using differential evolution. Energy Conv. Manage. 2009, 50(1): 97–104.

[47] Lu S, Sun C, and Lu Z. An improved quantum-behaved particle swarm optimization method for short-term combined economic emission hydrothermal scheduling. Energy Conv. Manage, 2010, 51(3): 561–71.

[48] Youlin Lu, Jianzhong Zhou, Hui Qin, Ying Wang, Yongchuan Zhang. A hybrid multi-objective cultural algorithm for short-term environmental/economic hydrothermal scheduling. Energy Conv. Manage. 2011, 52: 2121–2134.

Figure Captions

Fig. 1. Random points generated by (A) rank-1 lattice rule and (B) the ordinary MCS

Fig.2: Typical discretization of the probability distribution of the price forecast error

Fig. 3: The roulette wheel mechanism for the normalized probabilities of the price forecast levels

Fig. 4: Flowchart of the proposed scenario-based stochastic modeing of uncertainties

Fig.5: Piecewise linear emission generation curve with *M* prohibited zones

Fig. 6: Linear approximation of the absolute sinus function for valve loading effect

Fig. 7: Piecewise linear form of non-concave performance curves for hydro unit *j*

Fig. 8: Flowchart of the ε-constraint optimization method for the MMP problem

Table I: Results of the single objective HTSS problem

Single Objective	Profit ($)	Expected profit ($)	Emission (lbs)	Expected Emission (lbs)
Deterministic	2535224	-	161288	-
Stochastic	-	2528442	-	161134

Table II: 5 Pareto Optimal solutions of the deterministic multiobjective HTSS problem

Pareto Solution Number	F_1 : Profit ($)	F_2: Emission (lbs)
1	2535646.92	157420.36
5	2489486.32	124693.28
10	2378473.52	83784.42
15	2194129.43	42875.57
20	1899232.71	1966.71

Table III: Payoff table for the stochastic multiobjective HTSS problem

Objective Function	Minimum value of objective function	Maximum value of objective function
F_1 : Expected Profit ($)	1894347.22	2533858.45
F_2 : Expected Emission (lbs)	2171.61	158700.35

Table IV: Optimal solution of the stochastic multiobjective HTSS problem with equal weighting factors

Objective Function	Weighting factor	Objective function Value	Membership value
F_1 : Expected Profit ($)	1	2312199.39	0.653
F_2 : Expected Emission (lbs)	1	68078.44	0.579
Total membership of all objective functions			0.616

Table V: Optimal solution of the stochastic multiobjective HTSS problem with different weighting factors

Objective Function	Weighting factor	Objective function Value	Membership value
F_1 : Expected Profit ($)	3	2514601.40	0.970
F_2 : Expected Emission (lbs)	1	142223.64	0.105
Total membership of all objective functions			0.754

Table VI: Emission arbitrage for some of Pareto optimal solutions of the stochastic multiobjective HTSS problem

Total Expected Emission (lbs)	Expected Profit Without Emission Trade ($)	Expected Emission Trade ($)	Net expected profit ($)		
			$\pi^E = 1$ $/lbs	$\pi^E = 2$ $/lbs	$\pi^E = 3$ $/lbs
158700	2533858	-58700	**2475158***	2416458	2357757
133985	2499743	-33985	2465757	2431772	2397787
125747	2488137	-25747	2462390	**2436643***	2410896
109270	2450843	-9270	2441572	2432302	2423032
101032	2429995	-1032	2428963	2427932	**2426900***
92794	2403701	7206	2410907	2418114	2425320
2172	1894347	97828	1992176	2090004	2187832

Table VII: Optimization statistics for all four cases

Case	Variables	Discrete Variables	Equations	Solution time (Sec)
Case 1	16007	6714	19635	1.3
Case 2	160052	67117	196332	46.50
Case 3	384312	161136	471384	52.9
Case 4	3841392	1610808	4712112	6186

Table VIII. Scheduling results listed in [45-47]

Method	[45]	[46]	[47]
Fuel cost ($)	47906	44914	43507
Emission(lb)	26234	19615	18183

Table IX. Scheduling results listed in [48]

Schedule	HMOCA		NSGA-II		Schedule	HMOCA		NSGA-II		Schedule	HMOCA		NSGA-II	
index	F($)	E(lb)	F($)	E(lb)	index	F($)	E(lb)	F($)	E(lb)	index	F($)	E(lb)	F($)	E(lb)
1	41805	16841	42126	16763	11	43394	16243	43203	16404	21	45590	15943	44792	16109
2	41918	16731	42197	16773	12	43593	16204	43224	16372	22	45826	15915	45054	16065
3	42247	16542	42220	16770	13	43801	16174	43376	16338	23	46092	15887	45229	16053
4	42376	16494	42221	16766	14	44007	16140	43529	16302	24	46365	15867	45423	16037
5	42542	16452	42224	16680	15	44237	16108	43606	16270	25	46610	15844	45614	16021
6	42671	16395	42342	16636	16	44474	16076	43794	16240	26	46880	15815	45887	15995
7	42851	16357	42571	16592	17	44699	16049	44024	16217	27	47202	15794	46153	15967
8	42851	16357	42631	16542	18	44926	16021	44158	16195	28	47492	15772	46350	15947
9	43029	16313	42819	16511	19	45137	15995	44342	16170	29	47776	15755	46520	15934
10	43220	16276	42957	16449	20	45359	15968	44567	16140	30	481991	15746	46744	15914

Table X. Power generation of each unit in each hour using the proposed method

	Thermal Units (MW)			Hydro Units (MW)			
Hour/unit	1	2	3	1	2	3	4
1	96.59	176.00	188.68	80.55	50.16	28.99	129.03
2	106.76	188.23	196.83	80.44	51.30	30.71	125.74
3	81.24	157.55	176.40	78.79	52.93	31.47	121.63
4	65.79	138.98	164.03	77.00	54.50	33.87	115.82
5	66.54	139.88	164.63	75.36	55.50	37.01	131.08
6	97.95	177.64	189.77	75.47	57.53	40.97	160.68
7	132.68	219.40	217.57	76.21	60.62	44.19	199.32
8	142.77	231.53	225.65	76.65	62.64	43.59	227.16
9	160.57	252.94	239.89	77.80	65.45	42.63	250.72
10	151.41	241.92	232.56	78.53	67.22	41.78	266.59
11	152.98	243.81	233.82	79.82	69.32	40.69	279.57
12	167.77	261.60	245.65	80.34	71.18	39.62	283.83
13	153.97	245.00	234.61	80.38	71.65	39.21	285.19
14	127.28	212.90	213.25	80.14	72.18	37.73	286.53
15	119.84	203.95	207.29	79.84	73.58	37.01	288.50
16	134.02	221.01	218.65	79.91	75.22	40.06	291.14
17	128.87	214.81	214.52	78.80	75.51	43.81	293.67
18	149.71	239.88	231.20	78.56	76.13	47.43	297.09
19	132.14	218.75	217.14	76.50	76.45	50.17	298.86
20	123.09	207.86	209.89	74.94	77.52	52.66	304.04
21	77.53	153.09	173.43	72.11	78.14	54.72	300.99
22	61.48	133.80	160.58	71.22	79.58	56.61	296.72
23	59.04	130.87	158.63	72.45	79.74	58.01	291.26
24	44.39	113.26	146.89	73.80	78.26	59.00	284.4

Table XI.Comparison of CPU time for combined economic emission scheduling

Reference	[45]	[46]	[47]	[48]	Proposed method
Computation time (Sec)	1 h, 16 min and 22 sec	74.96 Sec	Not reported	Not reported	9.25 Sec

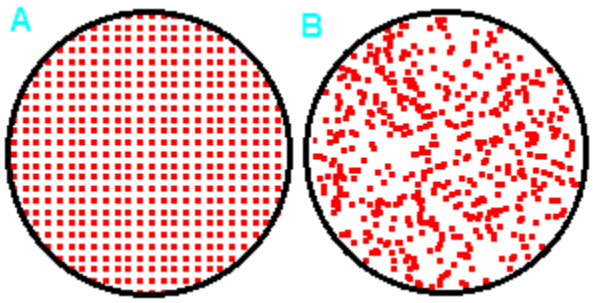

Fig. 1. Random points generated by (A) rank-1 lattice rule and (B) the ordinary MCS

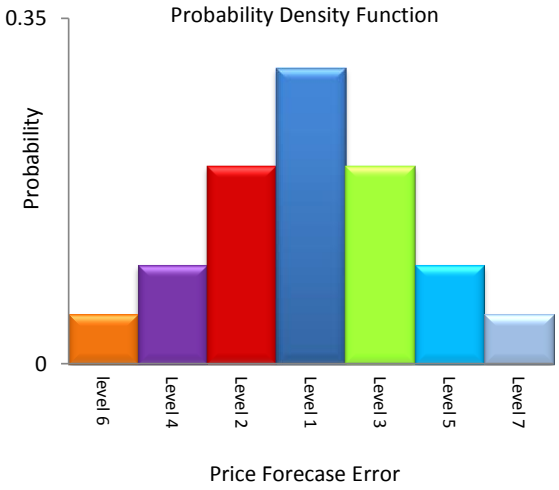

Fig.2: Typical discretization of the probability distribution of the price forecast error

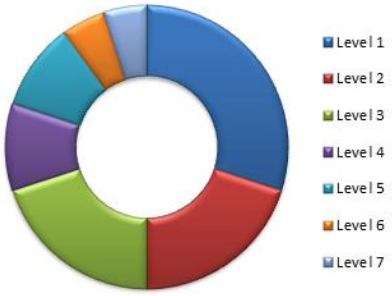

Fig. 3: The roulette wheel mechanism for the normalized probabilities of the price forecast levels

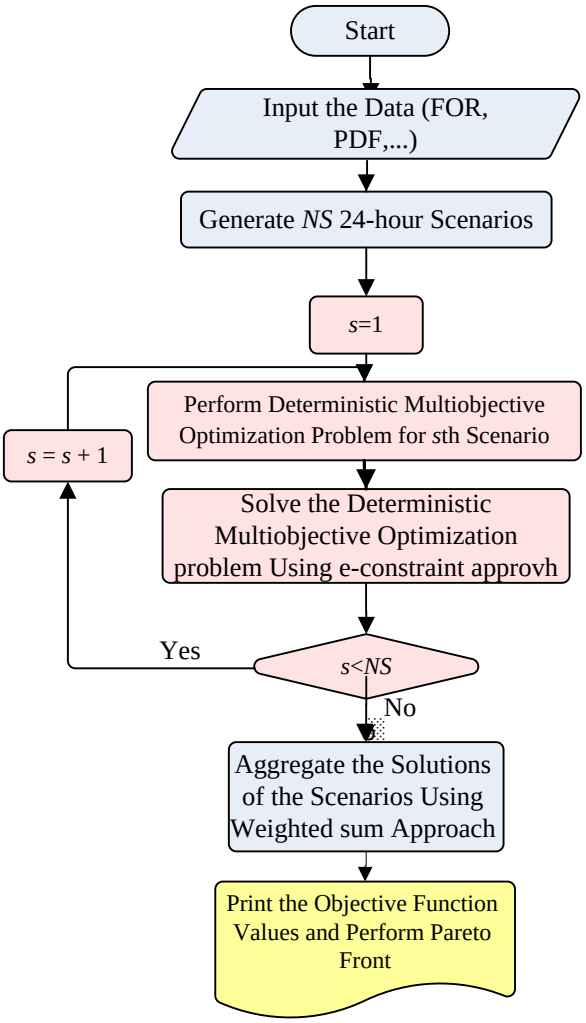

Fig. 4: Flowchart of the proposed scenario-based stochastic modeing of uncertainties

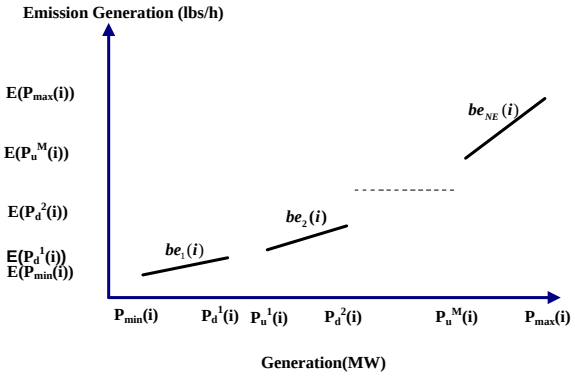

Fig.5: Piecewise linear emission generation curve with *M* prohibited zones

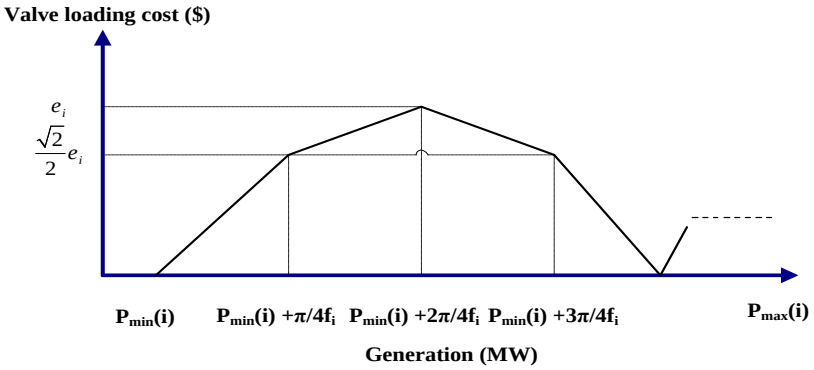

Fig. 6: Linear approximation of the absolute sinus function for valve loading effect

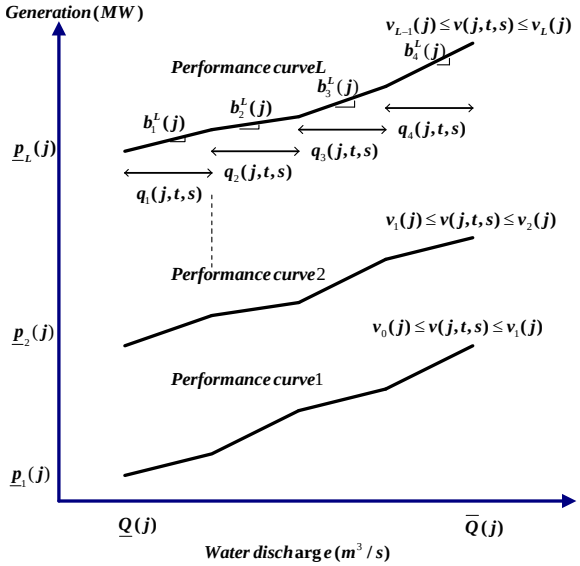

Fig. 7: Piecewise linear form of non-concave performance curves for hydro unit *j*

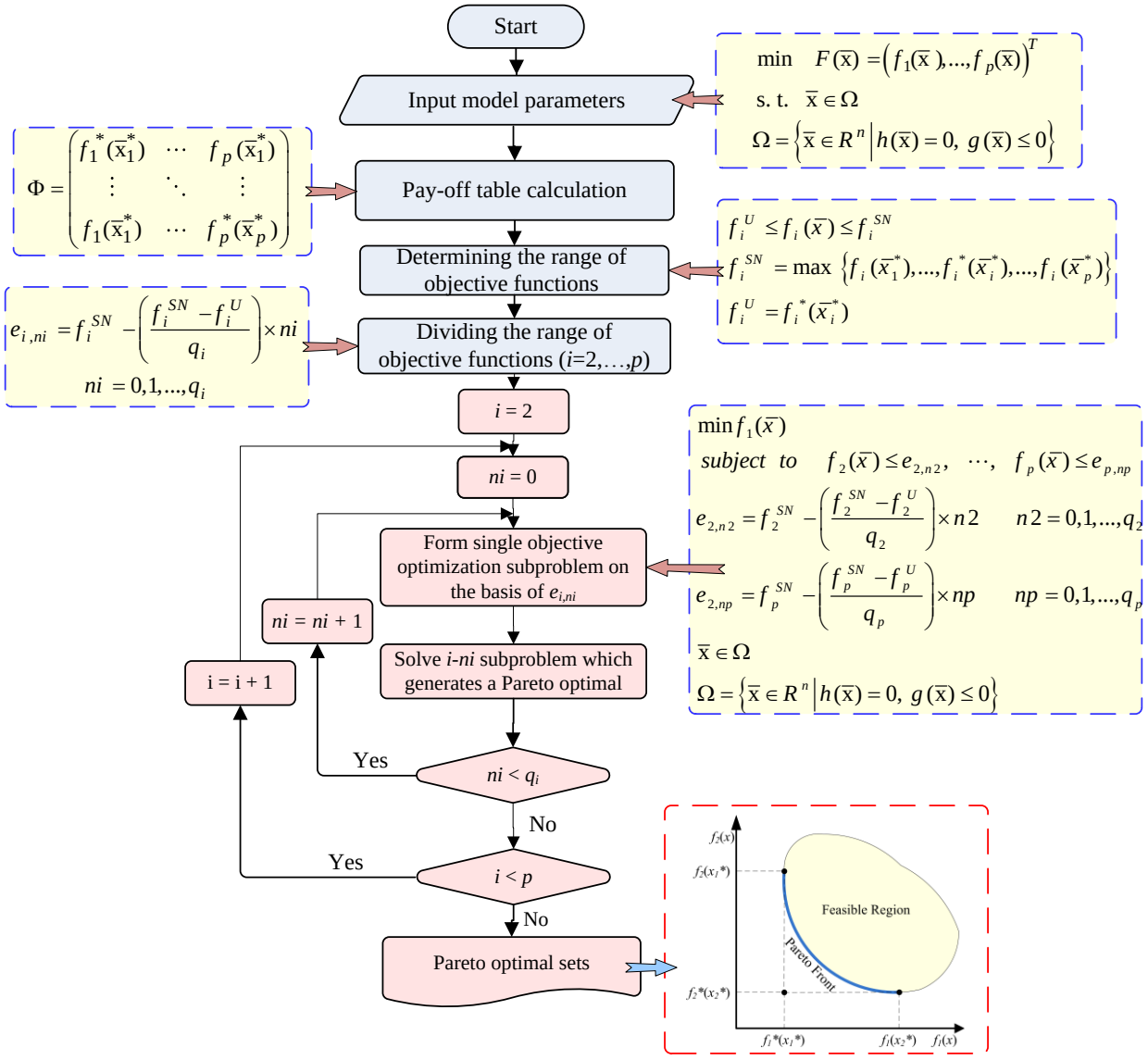

Fig. 8: Flowchart of the ε-constraint optimization method for the MMP problem